J. Math. Biol. (2000) 40: 64–96

Journal of Mathematical Biology

Models for spatial polymerization dynamics of rod-like polymers

Leah Edelstein-Keshet[1,*], **G. Bard Ermentrout**[2]

[1] Department of Mathematics, University of British Columbia, Vancouver, BC, Canada, V6T 1Z2. e-mail: keshet@math.ubc.ca
[2] Department of Mathematics, University of Pittsburgh, Pittsburgh, PA 15260, USA. e-mail: bard@math.pitt.edu

Received: 16 March 1999

Abstract. We investigate the polymerization kinetics of rod-like polymer filaments interacting with a distribution of monomer in one spatial dimension (e.g. along a narrow tube). We consider a variety of possible cases, including competition by the filament tips for the available monomer, and behaviour analogous to "treadmilling" in which the polymer adds subunits to one end and loses them at the other end so as to maintain a constant length. Applications to biological polymers such as actin filaments and microtubules are discussed.

Key words: Actin polymerization – Treadmilling – Spatial distribution of actin – Polymerization kinetics – Mathematical models

1. Introduction

The mathematical models described here arose as a result of our investigations into the polymerization kinetics of rod-like biological polymers such as actin and microtubules. Elsewhere, we have discussed how the addition or loss of monomers can influence the length distribution of a collection of polymer filaments (Edelstein-Keshet and Ermentrout, 1998; Ermentrout and Edelstein-Keshet, 1998). This paper focuses on how polymerization can influence the spatial distribution of the filaments.

For simplicity, we focus on a one-dimensional situation, in which all the polymers are aligned. Diffusional motion of the filaments

*To whom reprint requests should be addressed.

decreases rapidly as the filaments grow. Further, in biological examples, filaments are often tethered to each other or to other structures. Thus, we will ignore any relative motion of filaments and consider only polymerization and monomer diffusion in one dimension.

In many of the biological polymers, actin and tubulin included, the two ends of the polymer have distinct polymerization kinetics. Generally, one end grows considerably faster than the other. In actin, the barbed end (also called plus end) has faster kinetics than the pointed end (minus end). A similar situation holds for microtubules. Generally these biological polymers are oriented with the fast growing end pointed towards the membrane of the cell. This discrepancy in the kinetics is taken into account in our models.

To investigate the behaviour of the rod-like polymer in the presence of monomer we consider a variety of limiting cases, including those in which diffusion of the monomer is very fast. It is found that the presence of boundaries and conditions at the boundaries can affect the type of behaviour that is seen. Interpretation for the biological cases is considered.

Much of the discussion would apply in the general case of 1-D rod-like polymers. We have adopted some of the terminology used for actin for convenience of the notation, which is summarized below.

2. Glossary of parameters

A	Total amount of polymer in all forms
$a(x, t)$	The concentration of monomer at position x and time t
k_b^+	Polymerization rate constant for the fast growing "barbed" end of filament
k_b^-	Depolymerization rate for the fast growing "barbed" end of filament
k_p^+	Polymerization rate constant for the slow growing "pointed" end of filament
k_p^-	Depolymerization rate for the slow growing "pointed" end of filament
a_b	$= k_b^-/k_b^+$ Critical concentration for barbed end
a_p	$= k_p^-/k_p^+$ Critical concentration for pointed end
v	The incremental length of a polymer added by a single monomer
γ	The change in monomer concentration resulting from growth of a filament
n	Number of filaments in a filament bundle
$x_b(t)$	Position of a barbed end of a filament

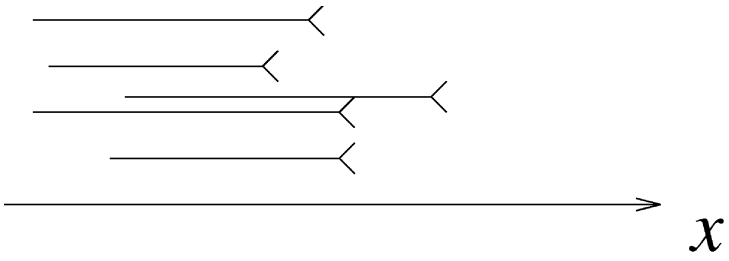

Fig. 1. The 1D geometry assumed in the models below: all polymer filaments are assumed to be rod-like, aligned along a common axis, and with the fast-growing ends of the polymer (represented as "barbed ends" in the diagram) pointing towards the positive x axis. (The barbs are only meant to distinguish front from back; we are not considering branched polymers.)

$x_p(t)$	Position of a pointed end of a filament
$\ell(t)$	Length of a polymer filament
$x_c(t)$	Position of the center of mass of a polymer filament
$r_b(t)$	Net rate of polymerization at the barbed end of a filament
$r_p(t)$	Net rate of polymerization at the pointed end of a filament
$v_b(t)$	Apparent rate of motion of the barbed end of a filament
$v_p(t)$	Apparent rate of motion of the pointed end of a filament

3. The model equations

Consider a single filament or a bundle of n filaments with their ends at the same position along the tube axis. (See Fig. 1, but consider the case that the pointed ends have the same x coordinate, and similarly for the barbed ends.) Let $x_b(t)$ and $x_p(t)$ be the spatial coordinates of the barbed and pointed ends, respectively, at time t. The ends will appear to move as monomer polymerization or dissociation occur. The apparent velocity (v_b, v_p) of these ends will be:

$$\frac{dx_b}{dt} = v_b = vr_b = v(k_b^+ a(x_b, t) - k_b^-), \tag{1}$$

$$\frac{dx_p}{dt} = v_p = -vr_p = v(k_p^- - k_p^+ a(x_p, t)), \tag{2}$$

where a stands for the concentration of monomer at the prescribed position. A convenient unit to use for distances such as x_i is the micron (μ). To convert number of monomer subunits added or lost to the net elongation or shortening by a physical distance, we use the factor v, which represents the length per monomer.

When the monomer concentration is fixed, the equations describing the motion of the polymer ends are uncoupled and can be solved independently. When this is not the case, the equation for the monomer is a diffusion equation with sources and sinks at the ends of the polymer bundle.

$$\frac{\partial a}{\partial t} = D\frac{\partial^2 a}{\partial x^2} - \gamma n[\delta(x - x_p)v_p + \delta(x - x_b)v_b]. \tag{3}$$

Here n is the number of filaments in the bundle (so that $n\ \delta(x)$ has dimensions of tips per unit length) and γ is a constant that converts elongation of the filaments to a corresponding net change in the monomer concentration. γ depends on the dimensions of the tube since this affects how much monomer is available per unit length of the tube. It also depends on the size of the monomers, since we need to convert lengths of polymerization to number (and thus concentration) of monomers. For a tube of cross-sectional area A,

$$\gamma = \frac{1}{\eta v A}. \tag{4}$$

where η converts the concentration (given in μM) to monomers per μ^3. (One finds that $\eta = 602$.) See the Appendix for the details and dimensional consistency of this formulation. Since polymerization is assumed to occur at the ends, the filaments only interact with the monomer profile at x_p and x_b.

There are other equivalent ways of presenting the model. From the units for the polymerization rate constants, it is apparent that certain ratios of parameters play a role in determining the balance between growth and shortening of a polymer. The following ratios have units of concentration

$$\frac{k_b^-}{k_b^+} = a_b,$$

$$\frac{k_p^-}{k_p^+} = a_p.$$

These are called the critical monomer concentrations for the barbed and pointed ends, respectively. We observe that equations (1) and (2) can be rewritten in terms of these as follows:

$$\frac{dx_b}{dt} = vk_b^+(a(x_b, t) - a_b), \tag{5}$$

$$\frac{dx_p}{dt} = vk_p^+(a_p - a(x_p, t)). \tag{6}$$

We also note that the problem can be treated from the point of view of the filament as a whole, namely its length, $\ell(t)$ and the position of its center of mass, $x_c(t)$. The formulation of the model in terms of $(x_b(t), x_p(t))$ or $(x_c(t), \ell(t))$ is interchangeable, but the equations are simpler in the former variables. We discuss the alternate formulation in the Appendix.

4. Fixed monomer distribution

As a first step, consider what happens if the monomer profile is artificially held fixed, with time-independent profile $a(x)$. Suppose a single filament is caught in this monomer profile. Then the equations for the positions of the filament ends can be solved in closed form.

4.1. Conditions for an immobile, static filament

The filament will appear to be fixed if the net rates of growth at each of the ends is zero ($r_b = r_p = 0$) i.e., if the monomer concentration at each end matches the given critical concentration at that end,

$$a(x_b) = a_b,$$

$$a(x_p) = a_p.$$

For the above conditions to be satisfied, the graph of the function $a(x)$ must intersect the values $a = a_p$ and $a = a_b$. With the given choice of coordinate system (barbed end towards the positive x axis), the intersection of $a(x)$ with the value a_b must be to the left of its intersection with a_p. For a fixed *stable* filament we must also impose conditions on the slope of the function $a(x)$ at the two endpoints. Consider a small perturbation which adds monomers to one of the ends of the filament. If this now places that end in a higher concentration, it will leave its equilibrium position and grow in length. The filament will be both fixed and stable, provided:

$$a'(x_b) < 0,$$

$$a'(x_p) > 0.$$

(The inequalities are opposite because polymerization at the pointed end leads to elongation in the negative x direction.) See Fig. 2 for a sketch of the appropriate configuration. For a smooth profile, the above conditions imply that a stable filament whose length and position are fixed would exist in a region in which the monomer profile has

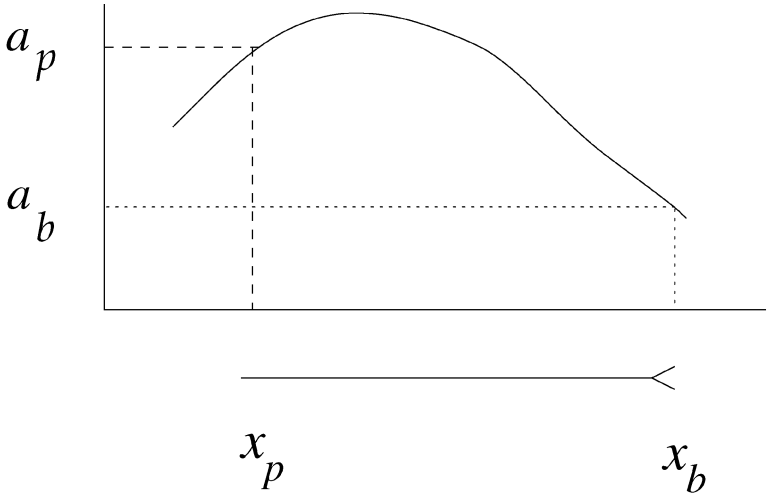

Fig. 2. A monomer profile which gives rise to a fixed filament length. The barbed ends and pointed ends must each be centered at their respective critical monomer concentration and the slope of the monomer gradient must be such that each tip is stable.

a local maximum. The length of the filament is then determined by the positions at which the monomer profile intersects the two critical levels.

4.2. Conditions for an elongating filament with fixed center of mass

A filament will appear to grow (or shrink) from a fixed center of mass when the rates of polymerization at the two ends are identical, i.e.

$$r_b = r_p.$$

Letting $\ell = x_p - x_b$, (and taking the center of mass of the filament to be at the origin, $x_p + x_b = 0$, without loss of generality), we find

$$k_b^+ a(\ell) - k_b^- = k_p^+ a(-\ell) - k_p^-. \tag{7}$$

In the Appendix we show that if this is to hold for all ℓ, and if the monomer profile is "very smooth" (i.e. the function $a(x)$ is analytic) then this situation can only occur in a spatially uniform monomer distribution whose level is

$$a = \left(\frac{k_b^- - k_p^-}{k_b^+ - k_p^+} \right). \tag{8}$$

(In the case of actin, whose rate constants are given in a later section, this level is roughly 0.06 μM, which is smaller than the critical

concentrations for both ends, so that the filament will be **depolymerizing**, and will disappear.)

4.3. Conditions for treadmilling

"Treadmilling" refers to the situation in which monomers are added at one end (the fast growing end) at the same rate as they are lost at the other (slow growing end). The length of the filament does not change, but the filament appears to move forward. This happens when

$$r_b = -r_p.$$

Two cases can be considered:

1. **Filaments of every length treadmill:** In this case, equation (7) must hold for every length ℓ. By using a Taylor expansion, we show in the Appendix that this situation can occur only if the monomer profile is uniform, and has the level

$$a = A_{tread} \equiv \left(\frac{k_b^- + k_p^-}{k_b^+ + k_p^+} \right). \tag{9}$$

   This constant monomer profile is the so-called **treadmilling concentration** (Wegner, 1982; Wanger et al., 1985; Kirschner, 1980; Selve and Wegner, 1986).
   The **treadmilling rate** is then given by

$$v_{tread} = k_b^+ A_{tread} - k_b^- = k_p^- - k_p^+ A_{tread} = \left(\frac{k_b^+ k_p^- - k_b^- k_p^+}{k_b^+ + k_p^+} \right). \tag{10}$$

2. **Only a specific length filament would treadmill:** In this case, we ask whether for some specific value of ℓ and corresponding monomer profile, a treadmilling solution is possible. The answer is positive, and we give further details of the monomer profile that results in the Appendix. We find an analytic expression that connects the filament length to the specific monomer profile that permits it to treadmill.

4.4. Treadmilling filament in equilibrium with fixed total pool

Now suppose that the total amount of the substance in all forms (monomers plus polymer) is fixed, and the monomer diffuses so rapidly that its spatial distribution is uniform. (This is a spatially independent case.) The connection between the monomer concentration a, (in micromolar concentration units, μM), the total amount of substance

in all forms, A (in μM) and the total length of polymer (expressed in micrometers, μ), is then given by the following conversion factor:

$$a = A - \gamma \ell,$$

where γ is the conversion factor previously defined in equation (4). The total length ℓ of the filament (or bundle) satisfies

$$\begin{aligned} \frac{d\ell}{dt} &= v((k_b^+ + k_p^+)a - (k_b^- + k_p^-)) \\ &= v((k_b^+ + k_p^+)(A - \gamma\ell) - (k_b^- + k_p^-)). \end{aligned}$$

Setting $d\ell/dt = 0$ and solving for ℓ we find that the steady state length of polymer is

$$\ell_{ss} = \frac{1}{\gamma}\left(A - \frac{k_b^- + k_p^-}{k_b^+ + k_p^+}\right) = \frac{1}{\gamma}(A - A_{tread}).$$

For the treadmilling steady state to occur, we must have $A > A_{tread}$. Further, it can be seen by simple substitution that $a = A - \gamma\ell_{ss} = A_{tread}$, i.e., the monomer level adjusts to match the treadmilling concentration. The rate of motion is then the treadmilling velocity, given previously in equation (10).

Based on the above, we can make the following observations:

- The rate of motion is independent of the total amount of substance, A.
- The total amount does, however, select the stable length of the treadmilling filament or filaments.
- Free monomers equilibrate at the treadmilling concentration. Any surplus of monomer is captured inside the filament.
- The rate of treadmilling can be affected by changes in the rate constants. Increasing k_b^+ or k_p^- will increase the speed of motion.
- Exactly the same results are obtained if there are n filaments in some bundle whose total length is ℓ rather than just one filament. The rate of motion is the same as before, the monomer concentration is the same, and the calculations hold exactly as before.

5. Treadmilling polymer bundle using up monomer

Dropping the assumption of a static monomer profile, we consider the dynamics of a single filament (or a filament bundle consisting of n filaments with tips together), "swimming" in a long 1D tube of monomer "fuel". The diffusion of monomer along the tube and its decay and production at the tips of the polymer is explicitly considered.

We assume that the tube is "infinitely long" with monomer held at a fixed concentration, α, at the two ends of the tube. We ask under what conditions the filament can treadmill at constant velocity, v, and how it would use up the monomers around it. Essentially, we look for a travelling wave solution to the full model, given by equations (1), (2), and (3).

As described above, the treadmilling case in which barbed and pointed ends are moving in the same direction with the same speed, i.e. $v_b = v_p = v$ corresponds to a filament of constant length (say ℓ) moving at constant velocity, v. We do not *a priori* specify the length of the filament or the treadmilling rate: these are to be predicted by the model. The boundary conditions are

$$a(x, t) \to \alpha \quad \text{for } x \to \pm \infty.$$

We look for travelling wave solutions with speed v. Transform coordinates by setting $z = x - vt$. Note that if we start with $x_b = 0$ at $t = 0$, we get from the last two equations above:

$$x_b = vt,$$

$$x_p = vt - \ell.$$

Thus,

$$x - x_b = x - vt = z,$$

$$x - x_p = x - vt + \ell = z + \ell.$$

Letting $\mathscr{A}(z) = a(x, t)$ be the monomer profile in the moving coordinate system, and using the above identities in the equation for the monomer concentration, we arrive at:

$$-v\mathscr{A}_z = D\mathscr{A}_{zz} + \gamma n[v\delta(z + \ell) - v\delta(z)].$$

Integrating once, we obtain

$$-v\mathscr{A} = D\mathscr{A}_z + \gamma n[vH(z + \ell) - vH(z)] + C,$$

where H is the Heaviside step function, and C is a constant of integration. In order to satisfy the boundary conditions, ($\mathscr{A} \to \alpha$, $\mathscr{A}_z \to 0$ for $z \to \pm \infty$) we set $C = -v\alpha$. The resulting equation is

$$D\mathscr{A}_z = n\gamma v(\alpha - \mathscr{A}) + n\gamma v\,(H(z) - H(z + \ell)).$$

This is a first order, linear ordinary differential equation with a discontinuous forcing term that turns "on" at $z = -\ell$ and turns "off" again at $z = 0$. We can solve this equation by integrating separately over each of the three regions $z < -\ell$, $-\ell < z < 0$, $z > 0$ and matching

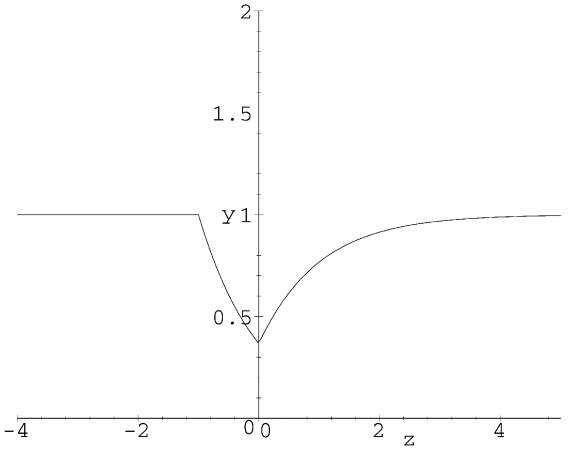

Fig. 3. A typical monomer profile in the case of a treadmilling filament consuming the monomer as it moves in one dimension. The explicit solution given by equations (11) is shown here with all constants set to unity ($v = D = \alpha = \ell = \gamma = 1$). The barbed end of the filament is at $z = 0$ and the pointed end at $z = -1$. The filament would move in the positive x axis, carrying with it this monomer profile.

the three solutions by imposing continuity at the points $z = -\ell, z = 0$. When this is done, we arrive at the solution

$$\mathscr{A}(z) = \begin{cases} \alpha & z < -\ell, \\ (\alpha - 1) + \mathrm{e}^{-n\gamma v(z+\ell)/D} & -\ell < z < 0, \\ \alpha - (1 - \mathrm{e}^{-n\gamma v\ell/D})\mathrm{e}^{-n\gamma vz/D} & z > 0 \end{cases} \tag{11}$$

The above solution reveals that the monomer profile is essentially "flat" at the back of the filament: the pointed end replenishes monomers by continual depolymerization. At the barbed end, there is a depression in the level of monomers due to consumption. The predicted monomer profile is shown in Fig. 3.

We can determine the velocity and length of the filament from the values of the monomer concentration at the ends of the filament: $\mathscr{A}(-\ell) = \alpha$, and $\mathscr{A}(0) = \alpha - (1 - \exp(-n\gamma v\ell/D))$. The velocity of treadmilling is given by the following two expressions, which must match to produce equal velocities at these two ends:

$$v = v_p = (k_p^- - k_p^+ \mathscr{A}(-\ell))v = (k_p^- - k_p^+ \alpha)v, \tag{12}$$

$$v = v_b = (k_b^+ \mathscr{A}(0) - k_b^-)v = (k_b^+(\alpha - (1 - \mathrm{e}^{-n\gamma v\ell/D})) - k_b^-)v. \tag{13}$$

From the first expression, we obtain a formula for the speed of treadmilling as a function of the supplied actin monomer level (but see

the restrictions on this level below). Setting the two expressions equal and solving for the length ℓ, we find that

$$\ell = \frac{D}{n\gamma v} \ln \Phi, \tag{14}$$

where

$$\Phi = \left(\frac{k_b^+}{k_b^+ + (k_p^- + k_b^-) - \alpha(k_p^+ + k_b^+)} \right). \tag{15}$$

Since the expression Φ is inside a logarithm, we must impose the condition

$$\Phi > 1,$$

in order for the length ℓ to be a real, positive quantity. This is equivalent to the condition

$$(k_p^- + k_b^-) - \alpha(k_p^+ + k_b^+) < 0$$

and leads to the inequality

$$\alpha > \frac{(k_p^- + k_b^-)}{(k_p^+ + k_b^+)} = A_{tread}.$$

The supplied monomer concentration must then, as expected, be greater then the concentration that permits treadmilling to occur. We also have the condition that the filament moves toward the positive x axis, thus

$$v = (k_p^- - k_p^+ \alpha) v > 0$$

which implies that

$$\alpha < \frac{k_p^-}{k_p^+} = a_p$$

so that the level of monomer supplied at the boundaries must be lower than the critical concentration for the pointed end of the filament. This is reasonable, since we are expecting that the pointed end will be losing monomers in the treadmilling case.

From the above calculations we can draw the following conclusions:

- A treadmilling solution in which monomers are consumed by a filament moving at steady velocity, v can only exist if the "supplied" monomer concentration (at the ends of the tube) is in a narrow range, above the treadmilling concentration and below the critical pointed end concentration. Outside of this range, no treadmilling solution can exist: either the filament elongates at both ends, or else it shrinks and disappears.
- The speed of the filament is proportional to the difference between the pointed end critical concentration and the supplied monomer

level. The greater the supplied monomer level (so long as it is still below a_p), the slower the speed of motion, since the required tendency towards depolymerization at the back of the filament is inhibited as the monomer level increases.

- The speed of the filament is further proportional to the pointed end depolymerization rate, which is a slow rate. Thus, as predicted in many papers in the literature, the treadmilling speed is limited by properties of the pointed end.
- The total length of the filament bundle is inversely proportional to the speed of motion. This would imply that a rapidly moving filament would tend to be shorter than a slow filament.
- The length of the filament that can treadmill in a given monomer level is proportional to the monomer diffusion rate. Since monomer diffusion is rapid, this would tend to favor very large filament lengths unless the treadmilling speed is very small.
- If $\alpha = a_p$, the velocity is zero and there is no treadmilling.
- if $\alpha = A_{tread}$ the above problem is also ill-defined, because any extension of the filament will drive the monomer level below A_{tread} and it will be unable to continue moving.

6. Competition of tips for monomer

In previous sections we investigated the case that one or more polymer filaments grow along a tube with their tips initially aligned. By assumption on the monomer diffusion, such tips feel the same level of monomer, and thus grow at the same rate. Hence, these tips stay together. We now consider what happens when several filaments are growing in the same tube, but with tips that start out at different positions. We ask how the interaction with the monomer distribution influences the relative positions of these tips, specifically, we want to determine whether the tips will get closer or further apart as a result of competition for the monomer.

We consider n filaments polymerizing inside a tube of constant, finite length, L, with the concentration of the monomer held fixed at the two ends of the tube. We will here investigate first the growth of barbed ends only, assuming that the pointed ends are held immobile at $x = 0$. At the boundaries, we assume that

$$a(0) = a(L) = \bar{a}.$$

The case of unequal concentrations at the two ends can be treated similarly. The question we investigate is whether, and under what conditions, barbed ends that are initially at different locations will get

closer or further apart from one another, and whether this will cause them to synchronize their motion. We show that the attraction/repulsion of tips depends both on the boundary conditions and the distance from the edge of the domain.

6.1. Monomer diffusion

For the monomer diffusion and polymerization/depolymerization at the filament ends we will assume that diffusion is sufficiently rapid compared to the other processes (tip growth) that we can consider the stationary form of the monomer diffusion equation:

$$0 = Da_{xx} - \gamma f(x),$$

where the function describing the depletion of monomer has the form

$$f(x) = \sum_{j=1}^{n} \delta(x - x_j)\,(k_b^+ a(x_j) - k_b^-),$$

(i.e. we have set $a_t = 0$ in the diffusion equation). Note that we now distinguish the positions of the tips, unlike our approach in equation (3) in which all the tips were assumed to have the same x coordinate.

The above equation describes the monomer profile resulting from rapid equilibration with the barbed ends using up monomers at positions, x_j, $j = 1 \ldots m$. The motion of the barbed ends, assumed slow in comparison with the monomer diffusion, follows the equation

$$\frac{dx_j}{dt} = v(k_b^+ a(x_j) - k_b^-). \tag{16}$$

By letting $a(x) = \bar{a} + \tilde{a}(x)$ we obtain simpler equations with homogeneous boundary conditions

$$a(0) = a(L) = 0,$$

and with a in equation (16) replaced by $\bar{a} + \tilde{a}$.

If the positions of the barbed ends are known at a given time, then the equation for monomer can be solved. The Green's function method proves to be suitable, since tips act as point-like sink singularities. We show in the Appendix that the appropriate Green's function for the problem with the given boundary conditions is:

$$G(x, y) = \frac{\gamma}{D}\left[\left(\frac{y}{L} - 1\right) x + H(x - y)\,(x - y)\right].$$

Then by the Green's function method, we have the solution

$$a(x) = \int_0^L G(x, y) f(y)\, dy = \int_0^L G(x, y) \sum_{j=1}^{n} \delta(y - x_j)(k_b^+ a(x_j) - k_b^-)\, dy.$$

The only contributions to the above integral occur when $y = x_j$, and this results in

$$a(x) = \sum_{j=1}^{n} (k_b^+ a(x_j) - k_b^-) G(x, x_j).$$

Plugging in the form for the Green's function, and including the superimposed homogeneous solution, we find that the monomer distribution is given by:

$$a(x) = \frac{\gamma}{D} \sum_{j=1}^{n} (k_b^+ a(x_j) - k_b^-) \left[\left(\frac{x_j}{L} - 1 \right) x + H(x - x_j)(x - x_j) \right] + \bar{a}.$$

In order to determine whether the tips that are ahead move faster or slower than those behind them, we would need to determine the monomer level at the position of the tip, i.e for the j'th tip at x_j we should compute $a(x_j)$ and compare to the levels felt by the other tips.

We now explicitly consider the case of two, three, or more barbed ends and make a further approximation to understand the relative velocities of the tips.

6.2. *Two interacting filaments*

Letting the number of filaments be $n = 2$ and using the form of the solution for the monomer distribution, we can determine $a(x_j)$, and hence also the velocity of growth $(k_b^+ a(x_j) - k_b^-)$, for each of the barbed ends shown in Fig. 4. In this case, the problem consists of a set of two

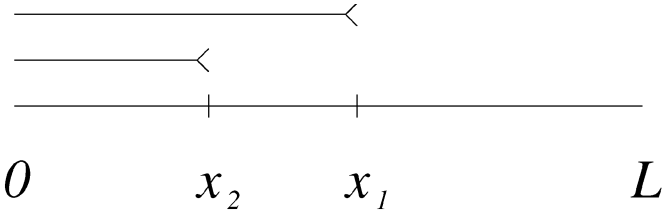

Fig. 4. Relative positions of two barbed ends polymerizing in a tube containing monomer with fixed monomer concentration at the ends of the domain. The shorter filament is predicted to move faster, and start to catch up with the longer one if the barbed ends both start out to the left of $L/2$.

coupled linear algebraic equations for the unknown monomer concentrations $a(x_1)$, $a(x_2)$. These equations can be solved fully in closed form. However, the precise values of $a(x_1)$, $a(x_2)$ are not particularly illuminating, since we are only interested in predicting which tip moves faster, i.e. in comparing their magnitudes. To do this, we can take a shortcut by assuming that the factors $(k_b^+ a(x_j) - k_b^-)$ in the equations are of a similar order of magnitude, $\approx (k_b^+ \bar{a} - k_b^-) = K$. This is equivalent to assuming that the monomer level is only changed a little by the presence of the tips, and that their relative positions contribute more heavily to the expressions in the large square brackets. Although this is only a first approximation, it is a convenient shortcut in comparing monomer concentrations at the tips.

Using this approximation, the concentration of monomer felt by the ith barbed end is

$$a(x_i) \approx \frac{K\gamma}{D} \sum_{j=1}^{n} \left[\left(\frac{x_j}{L} - 1 \right) x_i + H(x_i - x_j)(x_i - x_j) \right] + \bar{a}.$$

In the case of **two filaments** at positions x_1, x_2 with $x_1 - x_2 = d > 0$, we find that:

$$\begin{aligned} a_1 = a(x_1) &\approx \frac{K\gamma}{D} \left[\left(\frac{x_1}{L} - 1 \right) x_1 + \left(\frac{x_2}{L} - 1 \right) x_1 + d \right] + \bar{a} \\ &= \frac{K\gamma}{D} \left[\left(\frac{x_1 + x_2}{L} - 2 \right) x_1 + d \right], \\ a_2 = a(x_2) &\approx \frac{K\gamma}{D} \left[\left(\frac{x_1}{L} - 1 \right) x_2 + \left(\frac{x_2}{L} - 1 \right) x_2 + d \right] + \bar{a} \\ &= \frac{K\gamma}{D} \left[\left(\frac{x_1 + x_2}{L} - 2 \right) x_2 \right]. \end{aligned}$$

The tip at the back, i.e., at x_2 will catch up with the one at the front whenever it feels a slightly larger monomer concentration, i.e. when

$$a_2 > a_1$$

this occurs when

$$\left(\frac{x_1 + x_2}{L} - 2 \right) x_2 > \left(\frac{x_1 + x_2}{L} - 2 \right) x_1 + d$$

The inequality can be manipulated to yield

$$\left(2 - \frac{x_1 + x_2}{L} \right) (x_1 - x_2) > d$$

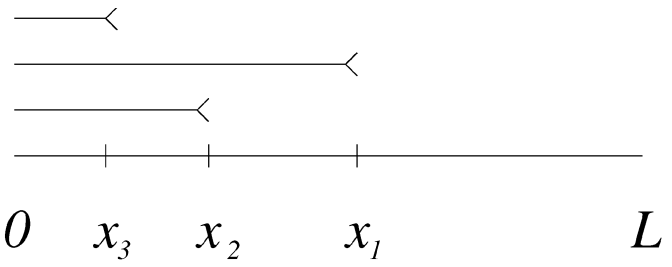

Fig. 5. Relative positions of three barbed ends. The distances between the tips are $d_{12} = x_1 - x_2$ and $d_{23} = x_2 - x_3$.

Using the fact that $x_1 - x_2 = d$ above, and simplifying, we find that

$$x_1 + x_2 < L$$

This inequality predicts that the tips will approach one another (so that the tip in the back will grow faster and get closer to the one in front) whenever the sum of the tip coordinates is smaller than L (or equivalently, the average of the tip coordinates is to the left of the domain midpoint.) Once the tips pass the midpoint of the domain, the leading tip should grow faster and leave the other behind.

6.3. Three or more filaments

The case of three filament ends can be handled similarly. Making the same approximation leads to a set of three expressions relating the concentrations felt by the tips at x_i to their positions as follows:

$$a(x_1) = K\left[\left(\frac{x_1 + x_2 + x_3}{L} - 3\right)x_1 + 2d_{12} + d_{23}\right],$$

$$a(x_2) = K\left[\left(\frac{x_1 + x_2 + x_3}{L} - 3\right)x_2 + d_{23}\right],$$

$$a(x_3) = K\left[\left(\frac{x_1 + x_2 + x_3}{L} - 3\right)x_3\right],$$

where $d_{12} = x_1 - x_2$ and $d_{23} = x_2 - x_3$ are the distances between the tips, assumed positive. (See Fig. 5.) It can be shown in a similar manner that the inequality $a(x_2) > a(x_1)$ is satisfied whenever

$$x_1 + x_2 + x_3 < L.$$

(When this is satisfied we also have $a(x_3) > a(x_2)$, so that the third tip catches up to the first two.)

Based on the above two examples, and using the same procedure, it follows that in the case of n filaments with barbed ends at $x_1 > x_2 > \cdots > x_n$, the tips will attract as long as

$$x_1 + x_2 + \cdots + x_n < L.$$

The calculations are identical, but more cumbersome in the general case. The conclusions from this analysis can be summarized as follows:

- In a finite tube of constant length with fixed monomer concentration at the two ends, the behaviour of a group of filaments is sensitive to their positions relative to the boundaries of the tube.
- If the n filament barbed ends are positioned so that their mean x coordinate is in the first L/n portion of the tube, the tips will get closer together and the filaments will appear to synchronize spatially.

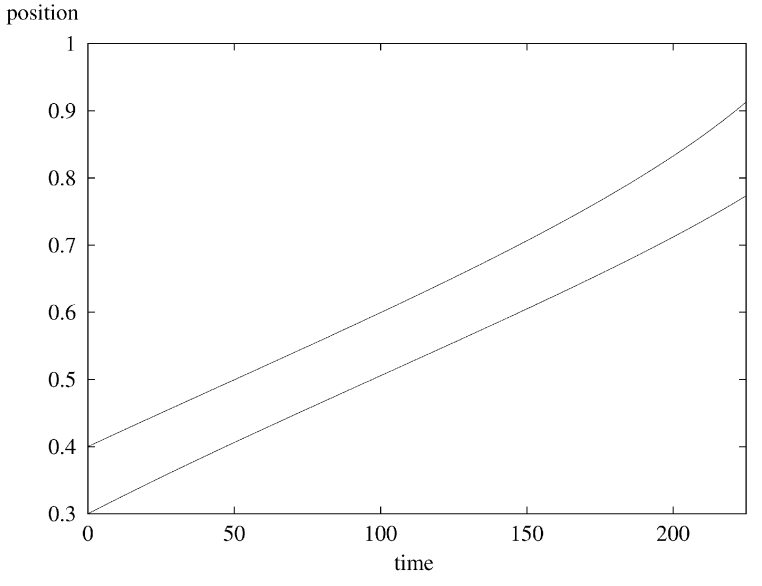

Fig. 6. The positions of two filament barbed ends $x_1(t), x_2(t)$ (vertical axis) as functions of time, t, (horizontal axis) are shown here as they grow in a domain of (dimensionless) length $L = 1$ starting with initial values $x_1(0) = 0.2$, $x_2(0) = 0.1$. Parameter values used were $\hat{\phi} = 0.00065$, $\beta = 4.2$, typical of actin polymerization dynamics–see Sect. 9. The monomer concentration at the boundaries was fixed at $\bar{a} = 10$. The domain was discretized with $N = 100$ points (grid spacing $h = 0.01$) for the PDE governing the monomer distribution. The filaments at first get closer to each other, but later recede, as shown magnified in the next figure.

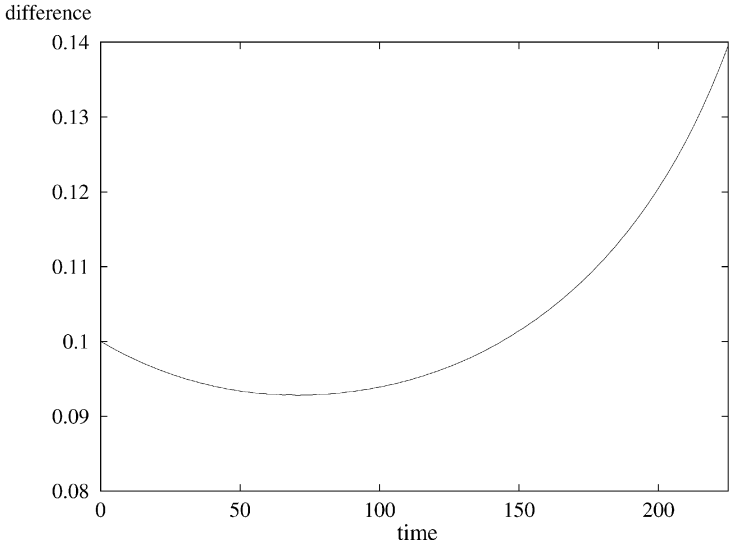

Fig. 7. The distance between the two barbed ends ($dx = x_1 - x_2$, vertical axis) is shown here as a function of time (horizontal axis). The positions of these tips was shown in Fig. 6. At first, the tips approach each other but as they cross the midpoint of the domain, they start getting further apart, as predicted by the steady state approximation. The parameter values are as in Fig. 6.

- As soon as the mean x coordinate falls outside this region, the leading tip will speed up and leave the other tips behind.
- The precise positions, speed, and dynamics of the tips is best seen with numerical simulations. See Figs. 6–8 for an example.

6.4. Numerical simulations of competing tips

To visualize the detailed dynamics of tip competition in the full model, and to test if our steady-state approximation for monomer is reasonable, we carried out simulations using the software **xpp** (which can be obtained free of charge from G.B. Ermentrout).

We considered the case of two tips, and used the full model, consisting of the following set of equations:

$$\frac{\partial a}{\partial t} = D\,\frac{\partial^2 a}{\partial x^2} + \sum_i k_b^+ \nu\gamma(a(x_i, t) - a_b)\,\delta(x_i),$$

$$\frac{dx_i}{dt} = \nu k_b^+ (a(x_i, t) - a_b), \quad i = 1, 2$$

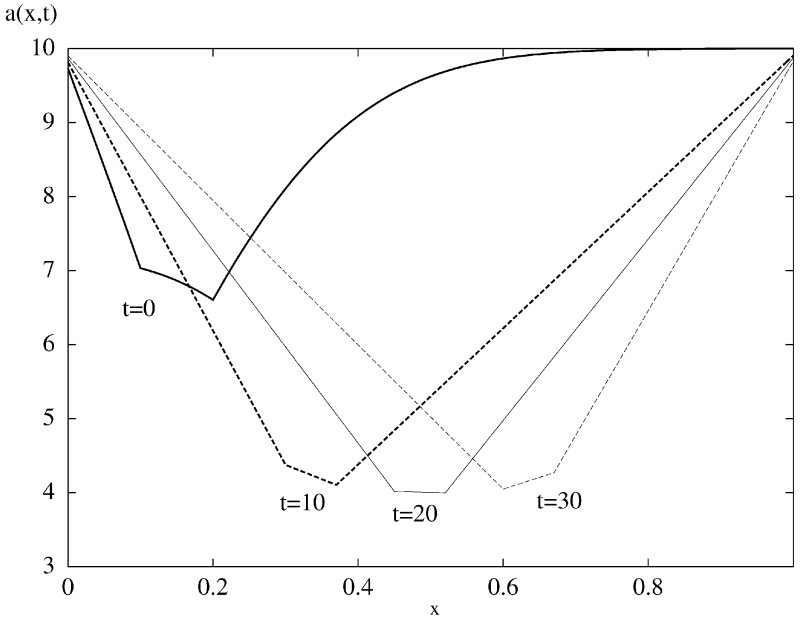

Fig. 8. A typical example of the monomer profile for the same conditions is shown at several times. Note that the boundary conditions are fixed at $a = \bar{a} = 10$ and the monomer concentration is initially $a(x, 0) = \bar{a} = 10$. The monomer distribution reveals a sink at the continually advancing positions of the two tips. This simulation can be interpreted as the polymerization dynamics of actin in a thin cellular appendage such as a filopodium – see Sect. 9 for details.

The equations were rewritten in dimensionless form by using the length of the domain, L, as the distance unit, the time to diffuse this distance, L^2/D as the time unit, and the critical concentration at the barbed end, $a_b = k_b^-/k_b^+$, as the concentration unit. Using these rescalings, it may be shown that the equations can be written in the form

$$\frac{\partial a}{\partial t} = \frac{\partial^2 a}{\partial x^2} + \sum_i \beta(a(x_i, t) - 1)\delta(x_i),$$

$$\frac{dx_i}{dt} = \hat{\phi}(a(x_i, t) - 1), \quad i = 1, 2$$

where

$$\beta = \frac{Lk_b^+(\gamma L)v}{D}, \qquad \hat{\phi} = \frac{Lk_b^- v}{D}.$$

with γ, v as previously defined. The values used in the simulations for the dimensionless parameters were derived from details of dynamics and geometry of structures associated with the polymer actin, leading

to $\beta \approx 4.2$, $\hat{\phi} = 0.00065$ for a tube of length $L = 10$ μ and radius about $r = 1.5$ μ. The domain (dimensionless size $= 1$ unit) was discretized with $h = 0.01$. The monomer concentration was assumed fixed and equal at the two boundaries, and the equations were solved numerically using the cvode option of **xpp**.

Results of these simulations are shown in Figs. 6–8. In Fig. 6, the positions of two barbed ends are shown traversing the domain. An enlarged view of the difference in their x coordinates in then shown in Fig. 7. It is evident from this figure that the tips get slightly closer to each other until they cross the midpoint of the domain, and thereafter get further apart, as predicted by our analysis using the steady state approximation for monomer. (The magnitude of the effect is not, however, large.)

We also show a profile of a typical monomer distribution which occurs for tips moving across a domain in Fig. 8. This profile shows how the tips of the filaments deplete monomer around them, and thus interact with other tips.

6.5. Growth on a semi-infinite domain

We consider a very long tube, and take as boundary conditions $a(0, t) = \bar{a}$ and $a(x, t) < \infty$. The equations are as before, but the Green's function is now:

$$G(x, y) = \bar{a} + \frac{\gamma}{D}[-x + H(x - y)(x - y)].$$

The problem is similar to the previous one, since we can solve for the monomer concentrations at the tips, or make a similar approximation to compare the magnitudes of monomer fuel concentration at the tips. This case is essentially parallel to the previous case, but with $L \to \infty$. Thus, it is not surprising to discover that the tips always attract and synchronize with one another, since their coordinates always satisfy

$$x_1 + x_2 + \cdots x_n < \infty.$$

7. Polymerization from monomer pool at one end

We have used a steady-state form of the monomer diffusion equation to investigate the behaviour of a filament or bundle of filaments under various polymerization conditions. In this section we consider one last example, in which a similar approach is applied.

In this example, monomers are supplied in concentrated form at $x = 0$, diffuse along the length of the tube, and polymerize at the barbed ends of a growing filament bundle. We assume, again, that the slow growing pointed ends are kept tethered at $x = 0$ and do not grow or use up monomer. This example bears similarity to the polymerization of actin in the acrosomal process of the sea cucumber, *Thyone* described experimentally by Tilney and Inoue (1982) and modelled in Oster et al. (1982) Oster and Perelson (1987) Perelson and Coutsias (1986). The mathematical analysis of this problem was discussed in Perelson and Coutsias (1986) and solved as a moving boundary Stefan problem. By using our simplified steady state approximation we can arrive at similar mathematical conclusions.

We let $a(x, t)$ denote the monomer concentration, L the length of the filament, and $a_0 = \bar{a}$ the concentration at the origin. The equations we consider are:

$$a_t = Da_{xx} - \gamma n v \delta(x - L)$$

where

$$\frac{dL}{dt} = v = vk^+(a(L, t) - a_b).$$

Following the method applied elsewhere in this paper, we assume the growth is slow compared to the diffusion so that the monomer distribution reaches steady state:

$$0 = Da_{xx} - \gamma n v \delta(x - L).$$

This equation can be integrated and solved yielding:

$$a(x) = \begin{cases} \bar{a} - (\gamma n v/D)\ x & \text{for } x < L, \\ \bar{a} - (\gamma n v/D)\ L & \text{for } x \geqq L \end{cases}$$

Setting $x = L$ and using the definition of v we find that

$$a(L) = \bar{a} - \tilde{C}L(a(L) - a_b),$$

where

$$\tilde{C} = \frac{\gamma n k^+ v}{D}$$

which we solve for $a(L)$ to get:

$$a(L) = \frac{\bar{a} + \tilde{C}La_b}{1 + \tilde{C}L}.$$

Substitute this into the differential equation for L:

$$\frac{dL}{dt} = vk^+\left(\frac{\bar{a} + \tilde{C}La_b}{(1 + \tilde{C}L)} - a_b\right)$$

After simplification, this leads to

$$\frac{dL}{dt} = vk^{+}\frac{(\bar{a} - a_b)}{(1 + \tilde{C}L)}$$

This can be solved using separation of variables, with the result

$$L(t) + \frac{\tilde{C}}{2} L^2(t) + \text{constant} = k^{+} v(\bar{a} - a_b)t. \tag{17}$$

By using the fact that $L(0) = 0$ we see that the constant in the above equation is just zero. Further, for large t (which implies large L), the quadratic term dominates on the left hand side so that. For t large,

$$\frac{L(t)^2}{t} \sim \frac{2}{\tilde{C}} k^{+} v(\bar{a} - a_b) = \frac{2D}{\gamma n}(\bar{a} - a_b)$$

so that the growth rate is dependent on the concentration difference, the number of tips, n, and the diffusion coefficient, but not on the rate constant. Estimation of various parameters in the case of the acrosomal process lead to the conclusion in the literature (that we also confirm) that diffusion is too slow (by a factor of about 10 according to Oster et al. (1982) and Oster and Perelson (1987) to account for the explosive growth of the actin bundle observed experimentally. (We do a similar calculation in the Appendix, and show that for a structure of diameter 0.05 μ and containing about 20 barbed ends at their tips, the ratio of L^2/t is roughly 30 μ^2/s). Recent personal communication with L. Tilney suggests that the number of barbed ends could be smaller – say about 20, that the diameter of the process may be up to 0.1 μ at its base, and that filaments may move relative to one another. This may account for part, (but perhaps not all) of the discrepancy between observed and diffusion-limited theory for L^2/t. (If the concentration of actin at the actomere is being underestimated by a factor of 2, the predictions would be in agreement with the observed rate of $L^2/t \approx 700\ \mu^2\, s^{-1}$, but this may be unlikely.) The hypothesis presented to account for the observed behaviour in the previous cited works was osmotic pressure.

8. Application to actin

In this section we describe one instance in which ideas presented in this paper could be applied, that of actin, a biological polymer and one of the major components of the **cellular cytoskeleton** (Alberts et al., 1989; Stossel, 1984). Actin is implicated in cell shape, motility, cell division,

Table 1. Typical values of parameters including polymerization rate constants and critical concentrations for actin filament

Parameter	Units	Value	Source
k_b^+	$\mu M^{-1} s^{-1}$	11.6	Pollard, 1986
		10	Carlier and Pantaloni, 1997
k_p^+	$\mu M^{-1} s^{-1}$	1.3	Pollard, 1986
		0.5	Carlier and Pantaloni, 1997
k_b^-	s^{-1}	1.4	Pollard, 1986
k_p^-	s^{-1}	0.8	Pollard, 1986
a_b	μM	0.12	
		0.08	Carlier and Pantaloni, 1997
a_p	μM	0.60	
		0.5	Carlier and Pantaloni, 1997
A_{tread}	μM	0.17	
		0.1	Carlier and Pantaloni, 1997
v_{tread}	s^{-1}	0.57	
		0.2	Carlier and Pantaloni, 1997
v	μ	2.7×10^{-3}	Spiros and Edelstein-Keshet, 1998
D	$\mu^2 s^{-1}$	50.0	Oster and Perelson, 1987
		90.0	Spiros and Edelstein-Keshet, 1998
η	$\mu^{-3}\ \mu M^{-1}$	620	Spiros and Edelstein-Keshet, 1998

and other vital functions. As assumed in this paper, an actin filament is rod-like for lengths up to a few microns; it is asymmetric, with ends having different polymerization kinetics. The **barbed end** (also called plus end) is most commonly associated with the membrane of the cell, while the **pointed end** (also called minus end) points into the interior of the cell (Tilney et al., 1981). The implications of this fact to treadmilling has been discussed in the literature (Kirschner, 1980; Selve and Wegner, 1986; Wanger et al., 1985; Wegner, 1982; Wang, 1985; Coluccio and Tilney, 1983).

Typical values for the rate constants associated with polymerization of actin are shown in Table 1. The critical concentrations at the two ends of an actin filament are: $a_b = k_b^-/k_b^+ \approx 0.12\ \mu M$, at the barbed end and $a_p = k_p^-/k_p^+ \approx 0.6\ \mu M$, at the pointed end.

In the literature, models for actin polymerization deal largely with total actin in polymerized versus monomeric form (Carlier and Pantaloni 1997) but see Oster et al. (1982), Oster and Perelson (1987), Oster and Perelson (1985) and, more recently, models in which actin-based polymerization ratchets provide the force driving motility (Mogilner and Oster 1996a, b). Many of these models include detailed consideration of mechanical forces and the interplay of chemistry with such

forces. In growing one-dimensional protrusions such as spikes, microvilli, stereocilia, and filopodia, the forward motion of the cytoskeleton in response to certain stimuli (e.g. Rehder and Cheng, 1998), or during developmental processes (Tilney and DeRosier, 1986; Tilney et al., 1991) implies that actin polymerization is taking place in a spatially controlled way. Similarly, intracellular parasites such as *Lysteria monocytogenes* see (Marchand et al., 1995), exploit actin polymerization to move through the cell. There are many features of the biological case which make the situation considerably more complex than has been described in this paper. In particular, actin interacts with many other proteins such as capping, fragmenting, sequestering, and bundling proteins that affect the way that it polymerizes.

For the purposes of the simplified models here, conversions from actin filament lengths to number of actin monomers are made as follows: There are 370 monomers in a 1 μ long filament. This implies that the parameter called v has the value $v = 1/370\ \mu = 2.7 \times 10^{-3}$ per monomer.

There are many cellular structures that act like the "thin tubes" discussed in this paper, so that the one dimensional geometry is suitable for such cases. Typical one-dimensional structures that contain actin filaments are cylindrical in shape with roughly the following dimensions: for stereocilia, which are appendages on hair cells in the auditory system, the diameter is $0.1 - 0.2\ \mu$ and the length is $1 - 5\ \mu$ (Tilney and DeRosier, 1986). For filopodia in neural growth cones, typical lengths are $10 - 25\ \mu$ (Rehder and Cheng 1998). For the acrosomal process of the sea cucumber, *Thyone*, the diameter is roughly $0.05\ \mu$ and the length is up to $90\ \mu$ (Oster and Perelson, 1987). A "typical" length for cellular appendages containing actin is therefore $10\ \mu$ and a typical diameter is $0.1\ \mu$; this leads to a crossectional area of $A \approx \pi(0.05)^2 = 0.00785\ \mu^3$. We also need the conversion between concentrations (quoted typically in μM) and monomers per μ^3. It can be shown (Spiros and Edelstein-Keshet, 1998) that 1 μM actin is equivalent to 602 monomers per μ^3. With these we find that

$$\gamma = \frac{1}{602\, vA} \approx 78.$$

For the parameters used in the numerical simulations, we compute

$$\beta = \frac{L^2 k_b^+ \gamma v}{D} = 4.2,$$

$$\hat{\phi} = \frac{L k_b^- v}{D} = 6.5 \times 10^{-4}.$$

We see from the simulations in Figs. 6 to 8 that for structures on the order of 10 μ, with parameters typical of actin polymerization, the phenomenon predicted in our analysis is apparent: namely, the barbed ends compete for monomer so that their relative speeds depends on their positions in the domain. This, of course, depends on the detailed boundary conditions and assumptions about the actin monomer that we have made: namely fixed concentration at the end of the domain, and level of monomer that can get depleted to some extent by the tips. The situation in vivo, i.e. in filopodia and stereocilia may not be the same in detail. It is still not known exactly how monomers are sequestered, and supplied. Moreover, it is unlikely that the boundary conditions we have used are appropriate for the biological situation. Thus, the simulations can not, at this stage, be considered as a model of the in vivo growth of filaments. Rather, they allow us to conclude that for lengths and parameters typical of actin filaments, the approximations made in the analysis hold fairly well in describing possible phenomena. Similar results (though not shown here) were obtained with domain size of 100 μ, the upper limit of the size of cellular appendages (e.g. the acrosome).

Treadmilling concentration: The possibility of treadmilling, and the treadmilling concentration for actin has been described throughout the literature (Wegner, 1982; Wanger et al., 1985; Kirschner 1980; Selve and Wegner 1986). For the typical parameters in Table 1, the treadmilling concentration is 0.17 μM using (Pollard, 1986) parameters, but 0.1 μM in (Carlier and Pantaloni, 1997). The **treadmilling rate** is given in Carlier and Pantaloni (1997) as $0.2\,s^{-1}$, whereas it is $0.57\,s^{-1}$ using rate constants from (Pollard 1986). The controversy in the literature about the relevance of treadmilling stems from the fact that these rates are much slower than could account for the motility of a typical cell.

Treadmilling in an infinite tube: The diffusion coefficient of an actin monomer is roughly $D = 5 \times 10^{-7}\,cm^2\,s^{-1} = 50\,\mu^2\,s^{-1}$. For an actin filament or bundle to treadmill in an "infinite tube" we must restrict the concentration of monomers in the tube to the range:

$$0.1 < \alpha < 0.5$$

For a typical value of $\alpha = 0.4$ μM, we find that $v = (k_p^- - k_p^+\alpha)v = 7.6 \times 10^{-4}\,\mu\,s^{-1} = 2.7\,\mu\,h^{-1}$. We also calculate that the value of Φ in equation (15) is roughly 1.3, so that the total length of polymerized actin in the treadmilling strand would be $\ell \approx 76.9/n$ from equation (14). For example, a strand consisting of 20 aligned actin filaments of length 3.8 μ each would undergo stable treadmilling in this actin concentration according to the predictions of the model. Methods of increasing filament growth rates (but not in the treadmilling case) have

been suggested in the recent literature (Carlier and Pantaloni 1997; Carlier et al., 1997; Dufort and Lumsden, 1996)

9. Application to microtubules

Microtubules, which are also components of the cytoskeleton are larger and stiffer than actin filaments, and have the shape of a hollow tube made up of α, β tubulin dimers, arranged in 12–16 protofilaments. For a review see (Walker et al., 1988; Hyams and Lloyd, 1994). The ends of a microtubule are called the plus (fast growing) and minus (slow growing) end. The polymerization kinetics of microtubules is somewhat more complex than that of actin. Aside from the usual addition and loss of monomers at each end, there is a rapid shortening state (represented below by k^-*) in which the polymer unravels very quickly. The transition from the normal state to the rapid shortening state is called catastrophe, and depends on the monomer concentration. The reverse transition, called rescue, is similarly monomer dependent. Parameters values typical for microtubule polymerization are given in the following table (Table 2).

Parameter values for microtubules polymerization: For the above parameters, if the microtubule is in the normal growth state, the treadmilling concentration is 5.075 μM. There are 1600 tubulin dimers per 1 μ in a microtubule. This implies that the treadmilling rate in length units is: $v = 7.3 \times 10^{-4}\,\mu\,s^{-1} = 2.6\,\mu\,h^{-1}$. A model which

Table 2. Typical rates of polymerization for microtubules as cited in (Walker et al., 1988). The subscripts "plus" and "minus" refer to the fast and slow ends, respectively, of the microtubule.

Parameter	Units	Value
k^+_{plus}	$\mu M^{-1}\,s^{-1}$	8.9
k^+_{minus}	$\mu M^{-1}\,s^{-1}$	4.3
k^-_{plus}	s^{-1}	44
k^-_{minus}	s^{-1}	23
k^{-*}_{plus}	s^{-1}	733
k^{-*}_{minus}	s^{-1}	915
a_{plus}	μM	4.94
a_{minus}	μM	5.35
A_{tread}	μM	5.075
v_{tread}	s^{-1}	1.167

describes the polymerization of microtubules would have to take into account the transitions that occur between the normal and the rapidly shortening states. A complete characterization of these transitions has been given in Walker et al. (1988).

10. Appendix

10.1. Dimensional considerations and units

Equations (1) and (2) are formulated in terms of length per unit time. The terms in brackets on the right hand sides have units of t^{-1}, and so the factor v carries dimensions of length. Equation (3) is formulated in terms of concentration per unit time, i.e. carries dimensions of $\mu M t^{-1}$. The terms $n\delta(x - x_i)$ have dimensions of a density per unit length. This follows from the observation that

$$\int_{-\infty}^{\infty} \delta(x - x_i)\, dx = 1$$

is dimensionless. Since v_i has units of μ/s, this implies that the conversion factor γ carries dimensions of concentration, i.e μM. To understand the detailed form of the conversion factor, note that $n\delta(x - x_i)$ is number of tips per unit length of the structure, $v_i \Delta t$ is the distance these move in time Δt and thus the total length of actin added per unit length of the structure. A factor of $1/v$ converts a filament length to the number of monomers added, a factor of $1/A$ converts this to a concentration of monomers polymerized per unit volume. Finally, a factor of η converts to a concentration in μM. This results in the expression $(1/v)\,(1/\eta)\,(1/A)\, n\delta(x - x_i)\, v_i$. Collecting the first three coefficients, we define the parameter γ as in equation (4). It can be verified that, thus defined, γ has units of μM.

10.2. Connection between coordinates of filament ends and filament properties

For $x_c(t)$ the center of mass (midpoint) of a filament and $\ell(t)$ its length, the positions of the two ends of the filament are

$$x_b(t) = x_c + \frac{\ell}{2},$$

$$x_p(t) = x_c - \frac{\ell}{2}.$$

The "position" x_c and the length ℓ satisfy the differential equations

$$\frac{d\ell}{dt} = r_b + r_p,$$

$$\frac{dx_c}{dt} = r_b - r_p.$$

where

$$r_b(t) = k_b^+ a\left(x_c + \frac{\ell}{2}\right) - k_b^-,$$

$$r_p(t) = k_p^+ a\left(x_c - \frac{\ell}{2}\right) - k_p^-.$$

i.e.,

$$\frac{d\ell}{dt} = k_b^+ a\left(x_c + \frac{\ell}{2}\right) - k_b^- + k_p^+ a\left(x_c - \frac{\ell}{2}\right) - k_p^-,$$

$$\frac{dx_c}{dt} = k_b^+ a\left(x_c + \frac{\ell}{2}\right) - k_b^- - k_p^+ a\left(x_c - \frac{\ell}{2}\right) - k_p^-.$$

10.3. Conditions for an elongating filament with fixed center of mass

Equation (7) can be restated in the form:

$$G(a(\ell) - a_b) = a(-\ell) - a_p$$

where the dimensionless parameter G is given by

$$G = \frac{k_b^+}{k_p^+}.$$

If the filament is to continue growing (or shrinking) uniformly, this equation must hold for all ℓ. Assuming that the monomer profile is analytic, we can expand $a(\ell)$ and $a(-\ell)$ in Taylor series about $x = 0$, obtaining

$$G\left(a_0 + a_1\ell + \frac{a_2}{2!}\ell^2 + \frac{a_3}{3!}\ell^3 + \cdots - a_b\right)$$

$$= \left((a_0 - a_1)\ell + \frac{a_2}{2!}\ell^2 - \frac{a_3}{3!}\ell^3 + \cdots - a_p\right),$$

where $a_j = a^{(j)}(0)$ is the j'th derivative of $a(x)$ at the origin. Equating term by term in the above expansion we obtain

- **Zeroth order:**

$$G(a_0 - a_b) = (a_0 - a_p).$$

- **jth order:**

$$(G-(-1)^j)a_j = 0.$$

Together these equations imply that in the "fixed filament center" case, if the monomer profile is analytic, then it must be spatially uniform i.e.

$$a(x) = a_0 = \left(\frac{Ga_b - a_p}{G-1}\right).$$

In terms of original parameters, this monomer concentration level is

$$a = \left(\frac{k_b^- - k_p^-}{k_b^+ - k_p^+}\right).$$

10.4. Conditions for treadmilling

The condition for treadmilling is equivalent to $dx_p/dt = dx_b/dt$. Assuming $x_b > x_p$, and setting $x_b = x_p + \ell$ where $\ell > 0$ is fixed, this implies that

$$G(a(x_p + \ell) - a_b) = -(a(x_p) - a_p) \tag{18}$$

10.4.1. Filaments of every length treadmill
In this case the equation (18) must hold for **every length** ℓ. A Taylor expansion of the equation about $x = x_p$ leads to

$$G\left(a_0 + a_1\ell + \frac{a_2}{2!}\ell^2 + \frac{a_3}{3!}\ell^3 + \cdots - a_b\right) = -(a_0 - a_p),$$

where $a_0 = a(x_p)$, $a_j = a^{(j)}(x_p)$. Following steps as in the previous section, we find that

$$a(x) = a_0 = \left(\frac{Ga_b + a_p}{G+1}\right),$$

or simply

$$a = A_{tread} \equiv \left(\frac{k_b^- + k_p^-}{k_b^+ + k_p^+}\right).$$

This treadmilling concentration will result in filaments of any length moving at constant speed.

10.4.2. Only a specific length filament would treadmill
In this case, the mathematical problem is to determine a function $a(x)$ such that, given a fixed value of ℓ, the following equation is satisfied:

$$a(x + \ell) = \alpha - Ba(x),$$

where

$$\alpha = \left(\frac{k_b^- + k_p^-}{k_b^+}\right), \qquad B = \left(\frac{k_p^+}{k_b^+}\right).$$

For a given ℓ, this is similar to a linear difference equation (but with terms along the x axis specified at discrete points separated by multiples of ℓ. We can find bounded solutions if we restrict the domain to the positive x axis. While this suggests looking for exponential solutions of the form

$$a(x) = a_0 + a_1 e^{-\lambda x},$$

this form leads to complex values of λ. We therefore take the alternate assumption that

$$a(x) = a_0 + a_1 e^{-\mu x} \cos \omega x,$$

where μ, ω are real. By plugging into the equation (18), we find that

$$a_0 = A_{tread}$$

and that, in order for a filament of a specific length ℓ to treadmill, the precise actin profile must be of the form

$$a(x) = A_{tread} + a_1 \left(\frac{k_p^+}{k_b^+}\right)^{x/\ell} \cos\left((2m-1)\,\pi\,\frac{x}{\ell}\right)$$

This means that the monomer concentration varies about A_{tread} sinusoidally, decaying with distance from the origin (since $k_p^+/k_b^+ < 1$). The period of the monomer variation is related to the length of the treadmilling filament. We must select the parameter a_1 so that $A_{tread} + a_1 < a_p$ and $A_{tread} - a_1 k_p^+/k_b^+ > a_b$ so that the filament will continue to move in the positive x direction. The speed of treadmilling will vary with position.

11. Green's function solution

The Green's function used in Sect. 6.1 is arrived at as follows:

Consider the steady state diffusion equation with a point source

$$a_{xx} = \delta(x - y),$$

Integrate the equation twice:

$$a_x = C + H(x - y),$$

$$a = Cx + d + (x - y)H(x - y),$$

where H is the Heaviside step function. Use the homogeneous boundary conditions $a(0) = 0$, $a(L) = 0$ to conclude that

$$d = 0,$$

$$C = -\frac{(L-y)}{L} H(L-y).$$

With the appropriate scaling to include the constants, the Green's function is then as described in Sect. 6.1.

11.1. Diffusion limited growth and acrosomal process

In Sect. 7 we found that the growth of length over time was governed by the equation (17). Since the concentration of actin in the periacrosomal cup (at the source, i.e. at $x = 0$) is very large, (estimated to be $\bar{a} = 160 \times 1.3 \times 10^4$ monomers per cubic micron) we can neglect a_b. We use $D \approx 80\ \ \mu^2\,s^{-1}$, $n = 60$ tips, and a diameter of 0.05 μ for the acrosome to conclude (after suitable conversion to appropriate units) that

$$\frac{L^2}{t} = 2\ \times 80\left(\frac{\mu^2}{s}\right) \times 2.7 \times 10^{-3}(\mu) \times \frac{1}{60\ \text{tips}} \times \pi 0.025^2$$

$$\times 160 \times 1.3 \times 10^4 \left(\frac{\text{monomers}}{\mu^3}\right) \approx 30\,\frac{\mu^2}{s}$$

This is short by a factor of about 20 from the speed observed by Tilney and Inoue (1982). Changing the number of tips to 20 and the diameter to 0.1 μ accounts for a factor of 12, but does not quite cure the problem with the diffusion-limited theory.

References

Alberts, B., Bray, D., Lewis, J., Raff, M., Roberts, K., and Watson, J. D. 1989, Molecular Biology of the Cell, Garland, New York

Carlier, M., Laurent, V., Santolini, J., Melki, R., Didry, D., Xia, G., Hong, Y., Chua, N. and Pantaloni, D. 1997, Actin depolymerizing factor (ADF/Cofilin) enhances the rate of filament turnover: implications in actin-based motility, J. Cell Biol. **136**(6): 1307–1323

Carlier, M. and Pantaloni, D. 1997, Control of actin dynamics in cell motility, J. Mol. Biol. **269**: 459–467

Coluccio, L. M. and Tilney, L. G. 1983, Under physiological conditions actin disassembles slowly from the nonpreferred end of an actin filament, J. Cell Biol. **97**: 1629–1634

Dufort, P. A. and Lumsden, C. J. 1996, How profilin/barbed-end synergy controls actin polymerization: a kinetic model of the ATP hydrolysis circuit, Cell Motil. Cytoskel. **35**: 309–330

Edelstein-Keshet, L. and Ermentrout, G. B. 1998, Models for the length distribution of actin filaments I: Simple polymerization and fragmentation, Bull. Math. Biol. **60**(3): 449–475

Ermentrout, G. B. and Edelstein-Keshet, L. 1988, Models for the length distribution of actin filaments II: Polymerization and fragmentation by gelsolin acting together, Bull Math. Biol. **60**(3). 477–503

Hyams, J. S. and Lloyd, C. W. (eds.) 1994, Microtubules, Wiley Liss, New York

Kirschner, M. W. 1980, Implications of treadmilling for the stability and polarity of actin and tubulin polymers in vivo, J. Cell Biol. **86**: 330–334

Marchand, J., Moreau, P., Paoletti, A., Cossart, P., Carlier, M., and Pantaloni, D. 1995, Actin-based movement of Listeria monocytogenes: actin assembly results from the local maintenance of uncapped filament barbed ends at the bacterium surface, J. Cell Biol. **130**: 331–343

Mogilner, A. and Oster, G. 1996a, Cell motility driven by actin polymerization, Biophys. J. **71**: 3030–3045

Mogilner, A. and Oster, G. 1996b, The physics of lamellipodial protrusion, Eur. Biophys. J. **25**: 47–53

Oster, G. F. and Perelson, A. 1985, Cell spreading and motility: a model lamellipod, J. Math. Biol. **21**: 383–388

Oster, G. F. and Perelson, A. S. 1987, The physics of cell motility, J. Cell Sci. Suppl. **8**: 35–54

Oster, G. F., Perelson, A. S., and Tilney, L. G. 1982, A mechanical model for elongation of the acrosomal process in Thyone sperm, J. Math. Biol. **15**: 259–265

Perelson, A. and Coutsias, E. 1986, A moving boundary model of acrosomal elongation, J. Math. Biol. **23**: 361–379

Pollard, T. D. 1986, Rate constants for the reactions of ATP- and ADP-actin with the ends of actin filaments, J. Cell Biol. **103 (6 pt 2)**: 2747–2754

Rehder, V. and Cheng, S. 1998, Autonomous regulation of growth cone filopodia, J. Neurobiol. **34**(2): 179–192

Selve, N. and Wegner, A. 1986, Rate of treadmilling of actin filaments in vitro, J. Mol. Biol. **187**: 627–631

Spiros, A. and Edelstein-Keshet, L. 1998, Testing a model for the dynamics of actin structures with biological parameter values, Bull. Math. Biol. **60**(2): 275–305

Stossel, T. P. 1984, Contribution of actin to the structure of the cytoplasmic matrix, J. Cell Biol. **1**(2): 15s–21s

Tilney, L. G., Bonder, E. M., and DeRosier, D. J. 1981, Actin filaments elongate from their membrane associated ends, J. Cell Biol. **90**: 485–494

Tilney, L. G., Cotanche, D. A., and Tilney, M. S. 1991, Actin filaments, stereocilia, and hair cells of the bird cochlea VI. How the number and arrangement of stereocilia are determined, Development **116**: 213–226

Tilney, L. G. and DeRosier, D. J. 1986, Actin filaments, stereocilia, and hair cells of the bird cochlea IV. How the actin filaments become organized in developing stereocilia and in the cuticular plate, Dev. Biol. **116**: 119–129

Tilney, L. G. and Inoue, S. 1982, Acrosomal reaction of Thyone sperm II. The kinetics and possible mechanism of acrosomal process elongation, J. Cell Biol. **93**: 820–827

Walker, R. A., O'Brien, E. T., Pryer, N. K., Soboeiro, M. F., Voter, W. A., Erickson, H. P., and Salmon, E. D. 1988, Dynamic instability of individual microtubules analyzed by video light microscopy: rate constants and transition frequencies, J. Cell Biol. **107**: 1437–1448

Wang, Y. 1985, Exchange of actin subunits at the leading edge of living fibroblasts: possible role of treadmilling, J. Cell Biol. **101**: 597–602

Wanger, M., Keiser, T., Neuhaus, J. and Wegner, A. 1985, The actin treadmill, Can J. Biochem. Cell Biol. **63**: 414–421

Wegner, A. 1982, Treadmilling of actin at physiological salt concentrations: an analysis of the critical concentrations of actin filaments, J. Mol. Biol. **161**: 607–615